Along the east coast of India, an early morning peak is observed and over the inland regions and the west coast, an afternoon/evening peaking is observed.

Fig. 6.3 shows hourly average rainfall during the NE monsoon season (Oct-Dec) showing the diurnal variation of observed rainfall over different stations over the south Peninsula. These plots are made using hourly station rainfall data, taken from the IMD archives. These plots clearly suggest that the stations over the east coast experience maximum rainfall during the morning hours. Over the interior parts and the west coast, maximum rainfall occurs during the evening and early night hours. Different physical mechanisms could be responsible for the observed rainfall diurnal variations over land and oceans. The observed rainfall peak in the late afternoon over the land could be due to intense surface solar heating and resultant convective instability. Over the east coast, the presence of a strong sea-land breeze is also noted to be responsible for diurnal variations (Bhate et al., 2019, Ramesh Reddy et al., 2021).

It is important to make a detailed analysis using Numerical Weather Prediction (NWP) model results, whether the NWP models are capable of predicting these observed diurnal variations. An analysis of diurnal variations for the southwest monsoon revealed that NWP model (WRF model) has constraints in predicting diurnal variations accurately (Bhat et al., 2019). The model was found successful in simulating the pattern of diurnal variation of rainfall, but underestimates its amplitude compared to the observed one especially over the western Himalayas, northeast India, central India, and the north Bay of Bengal (BoB). It is important to carry out an extensive analysis to examine how the NWP models are capable of predicting the diurnal variations of NE monsoon rainfall accurately.

6.2. **Intra-seasonal variation of NE monsoon rainfall**

Several studies have shown that during the southwest monsoon season (June to September) a substantial component of the variability of convection and rainfall over the Indian region arises from the fluctuations on the intra-seasonal scale between active

and weak or break spells (Ramamurthy, 1969; Goswami, 2005; Rajeevan et al., 2010). Long intense breaks are known to have an impact on the seasonal monsoon rainfall over the country (Webster et al., 1998; Gadgil and Joseph, 2003, Rajeevan et al., 2010). The dry and wet spells of the active and break conditions represent the sub-seasonal or intra-seasonal variations of the monsoon with timescales longer than synoptic activity (1–10 days) but shorter than a season.

Recent research results also provided new insights regarding the origin of the monsoon intra-seasonal variations. The ISOs of summer monsoon essentially have timescales between 10 and 90 days. Within the broad range of 10–90 day periods, two period ranges with periodicities between 10 and 20 days and 30 and 60 days respectively are particularly prominent (Goswami, 2005). Active and break spells and intra-seasonal variations of the Indian summer monsoon have been extensively studied. As far as the northeast monsoon is concerned, not much knowledge is available on the intra-seasonal activity during the NE monsoon season. Therefore, the results of the intra-seasonal activity during the northeast monsoon season are discussed in this section.

Fig. 6.4 shows daily rainfall (averaged over the NE monsoon region) from 15 September to 15 January during two sessions, 2008-2009 and 2011-2012. These plots clearly show that rainfall activity over the region is confined to only a few days during the season, which is interspaced between dry or weak monsoon spells. For example, during 2008-2009, heavier rainfall activity was observed around 20-30 October. The next rainfall activity was observed almost after one month, from 20 Nov onwards. Between 30 October to 20 November, rainfall activity over the region was generally subdued. Similar intra-seasonal variability of rainfall with enhanced (suppressed) activity was observed during 2011-12 also.

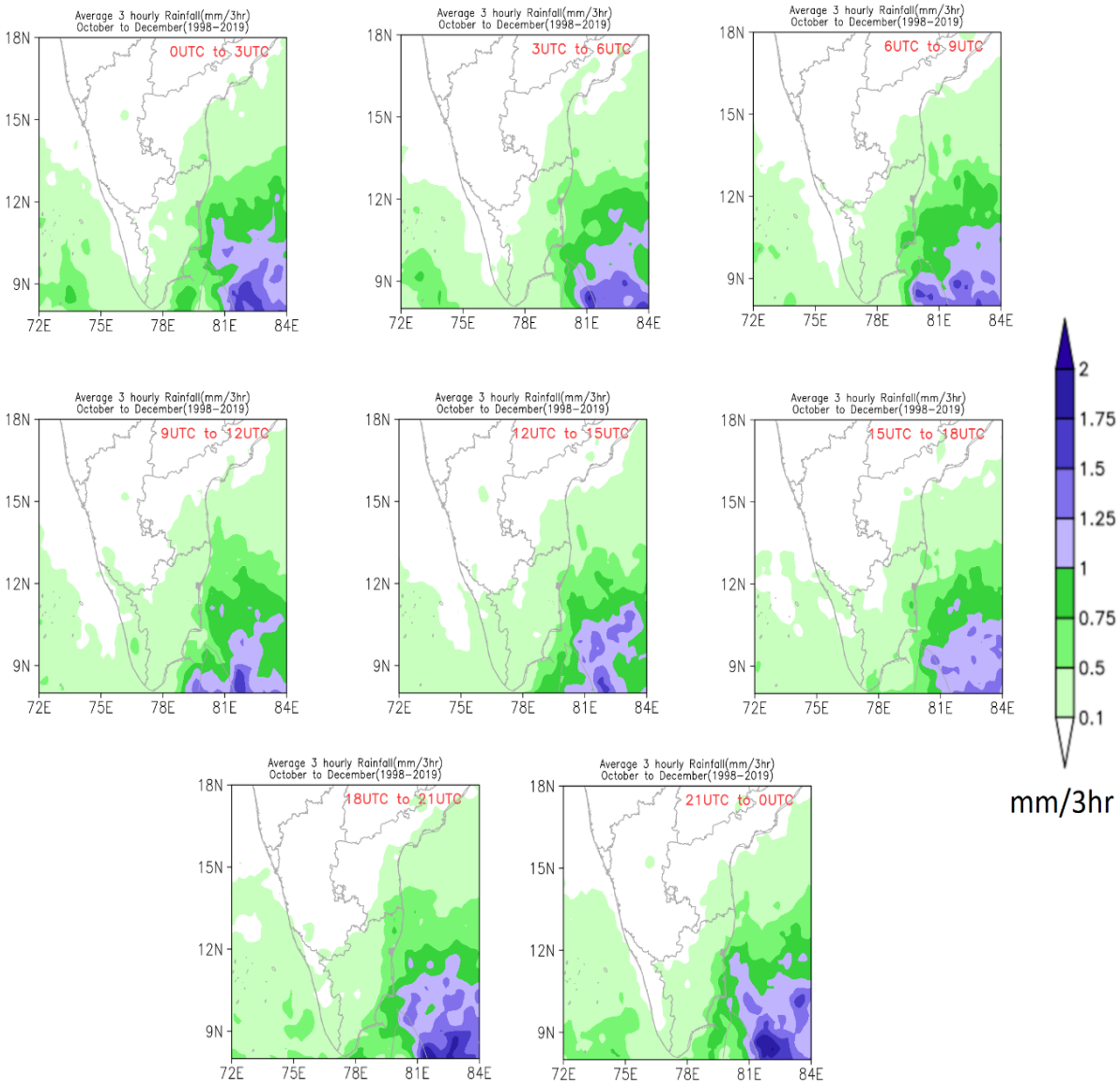

Fig. 6.1. Average 3-hourly seasonal (October to December) rainfall (mm/3h) over the Indian region averaged over the years 1998-2019 derived from the TRMM 3G68 data.

Fig. 6.5 a shows the Hovmuller diagram showing Outgoing Longwave Radiation (OLR) anomalies averaged over 70^0 -90^0E plotted with latitude versus time (15 Sept 1998 to 15 January 1999). Fig. 6.5 b shows the similar plot but for the period 15 Sept 2000 to 15 January 2001. OLR is a proxy for atmospheric convection. Low OLR suggests more convection. These two plots clearly show strong intra-seasonal activity during the NE

monsoon season. Fig 6.5 a shows clear northward propagation of OLR anomalies from the equator around 16 October and the next one around 15 November Another northward propagation is observed around 18 December. However, all the northward propagation of convections are limited to 15^0N only. During the southwest monsoon season, this northward propagation moves to even the foothills of the Himalaya. Fig 6.5 b shows a similar plot, but for zonal wind anomalies at 925 hPa. This plot clearly shows the strengthening of the shear zone (between westerlies in the south and easterlies in the north) at particular intervals. This plot also shows the slow southward movement of the horizontal wind shear zone by December, which represents the southward movement of ITCZ.

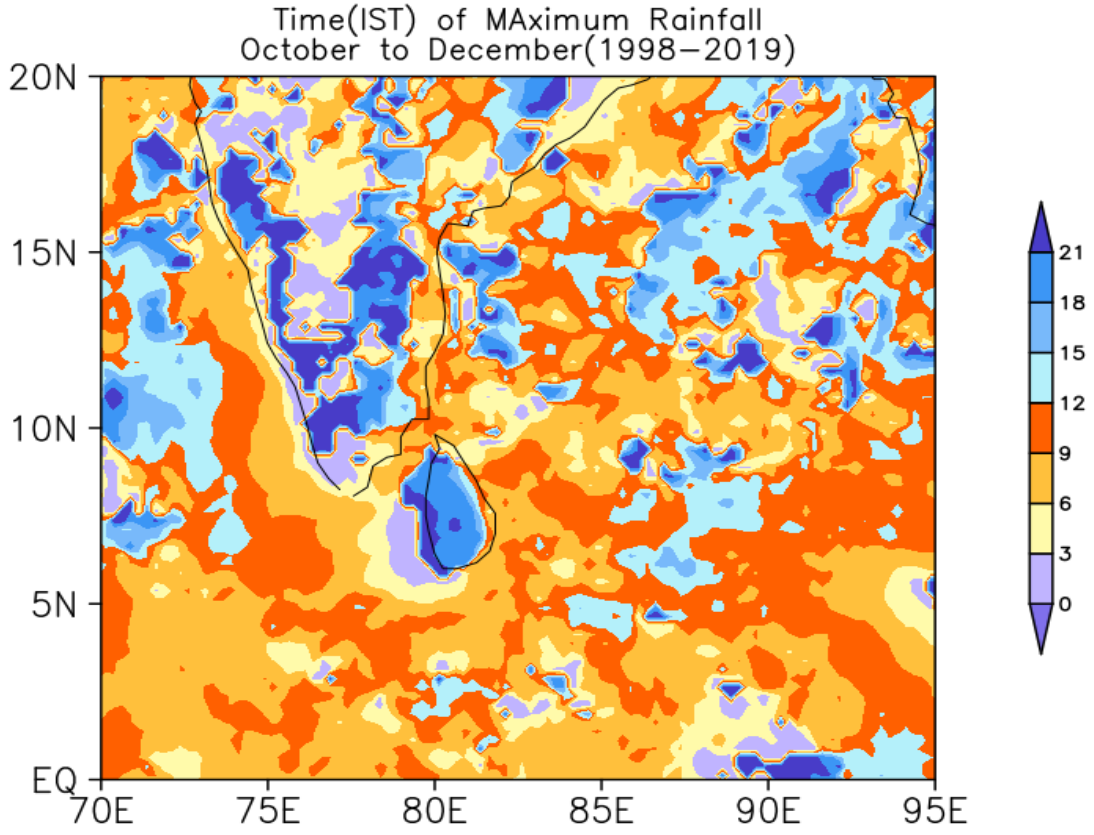

Fig. 6.2. Phase angle (time of maximum rainfall peak) in Indian Standard Time (IST) based on satellite data for the period using the Harmonic Analysis (1998-2019).

East Coast stations

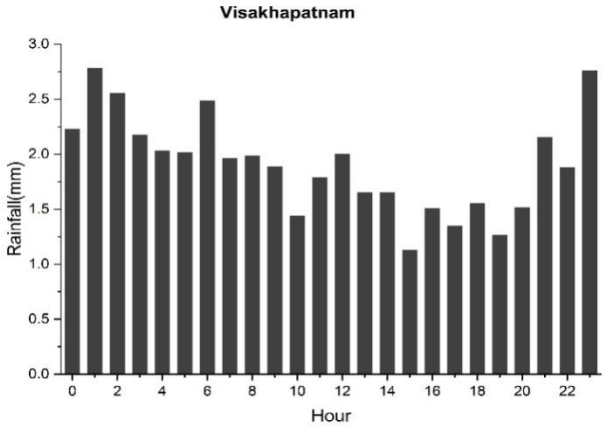

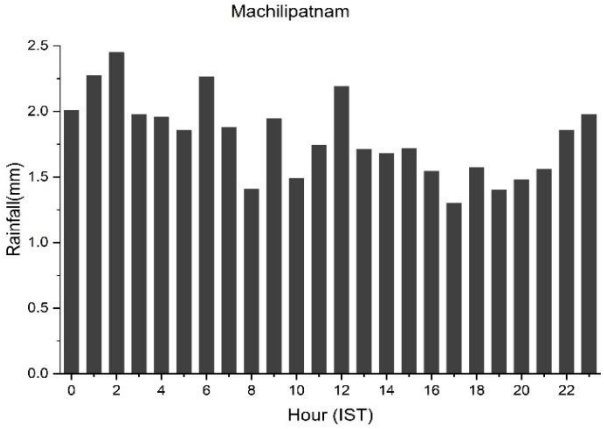

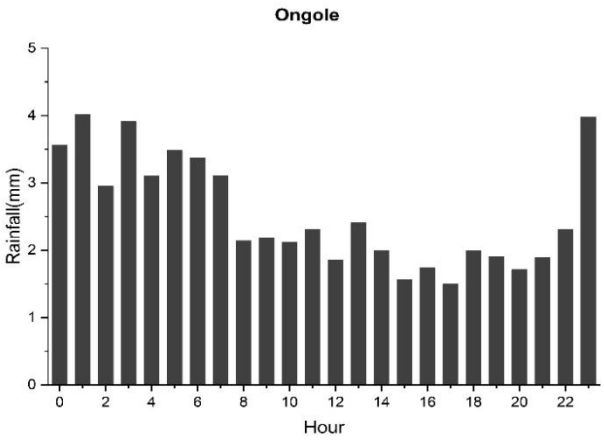

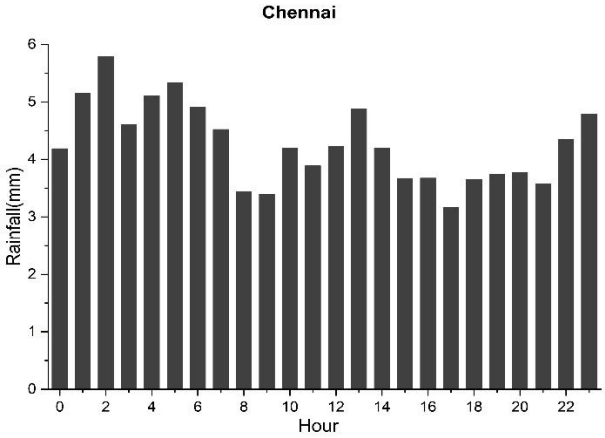

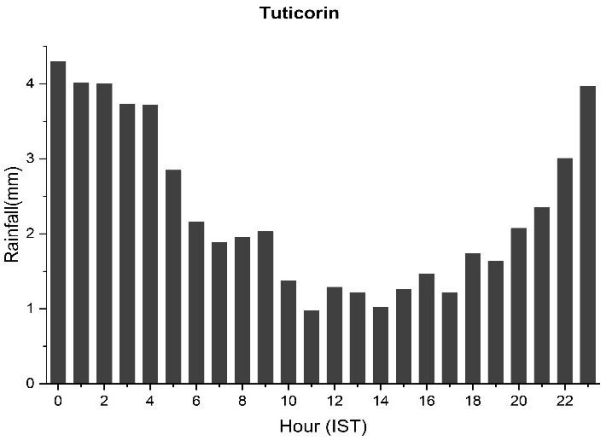

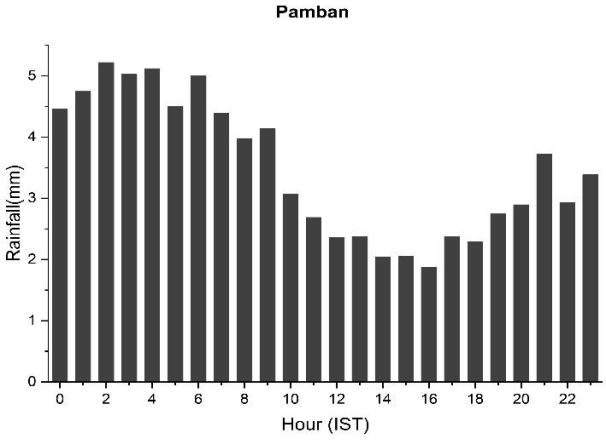

Central Region Stations

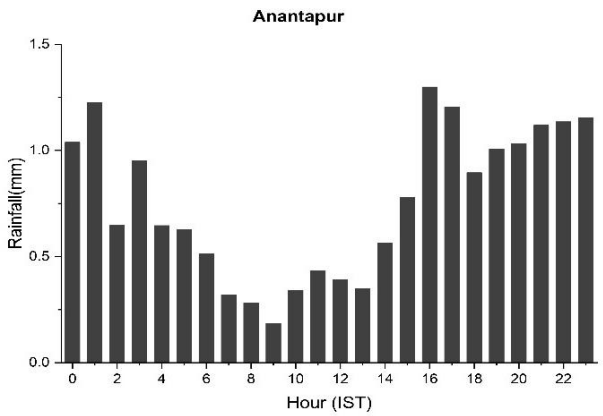

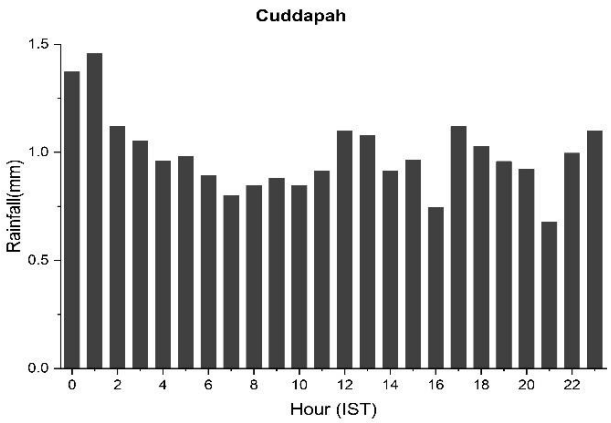

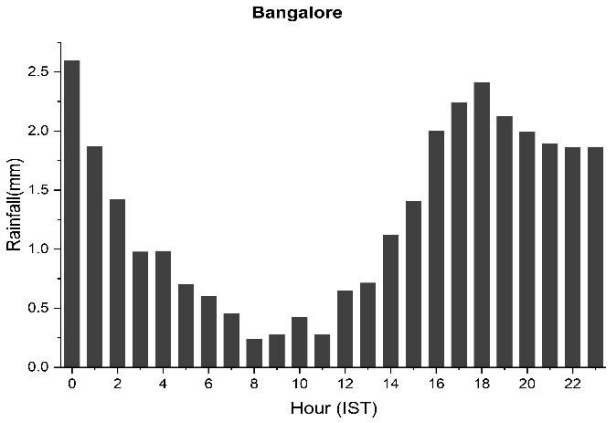

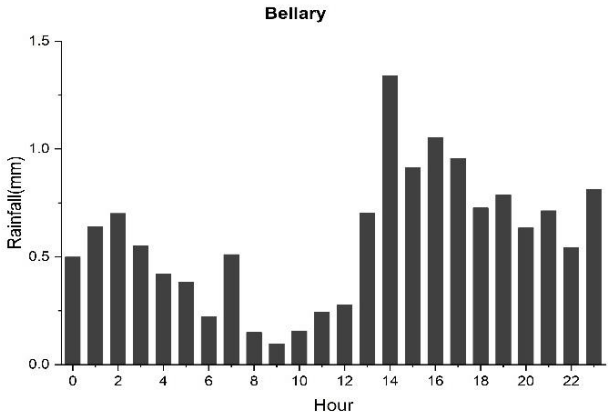

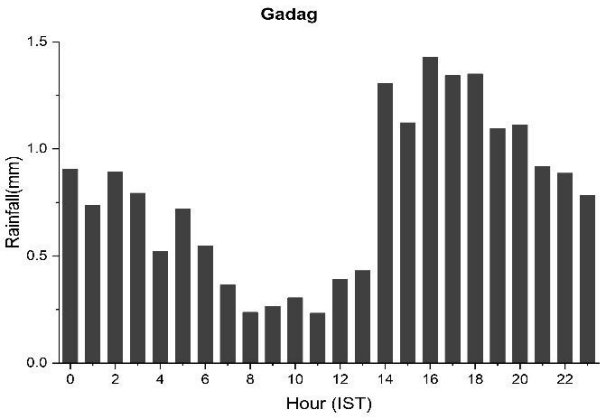

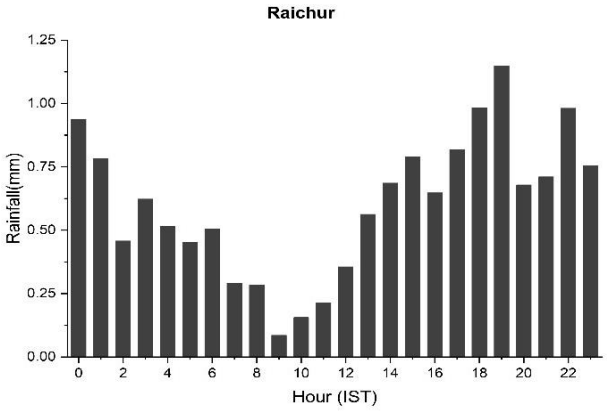

Central Region Stations

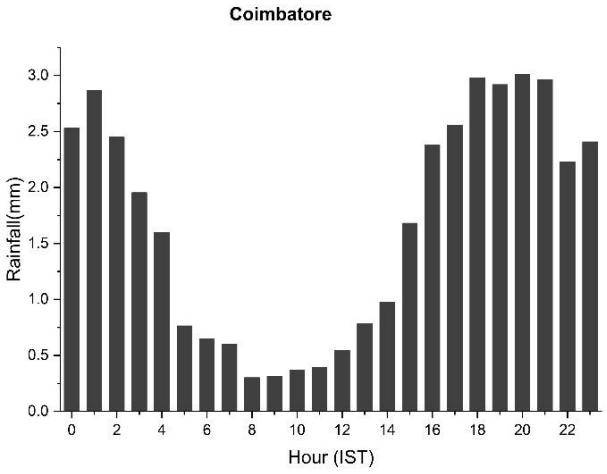

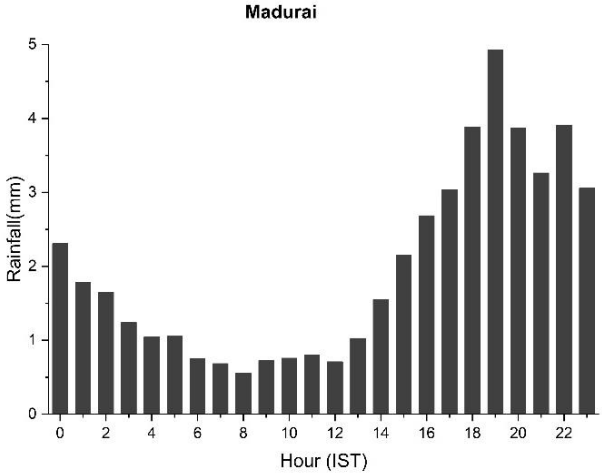

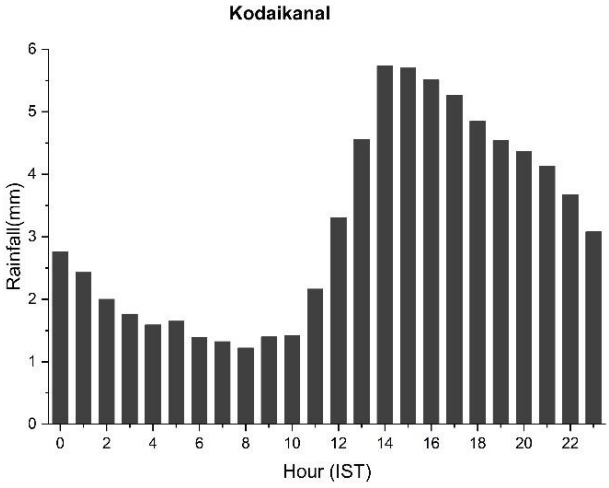

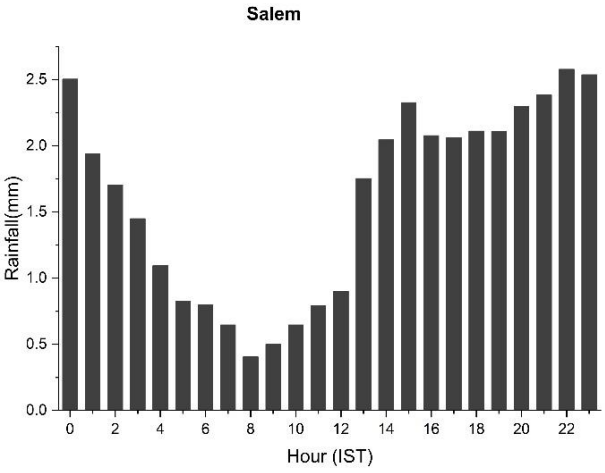

West Coast Stations

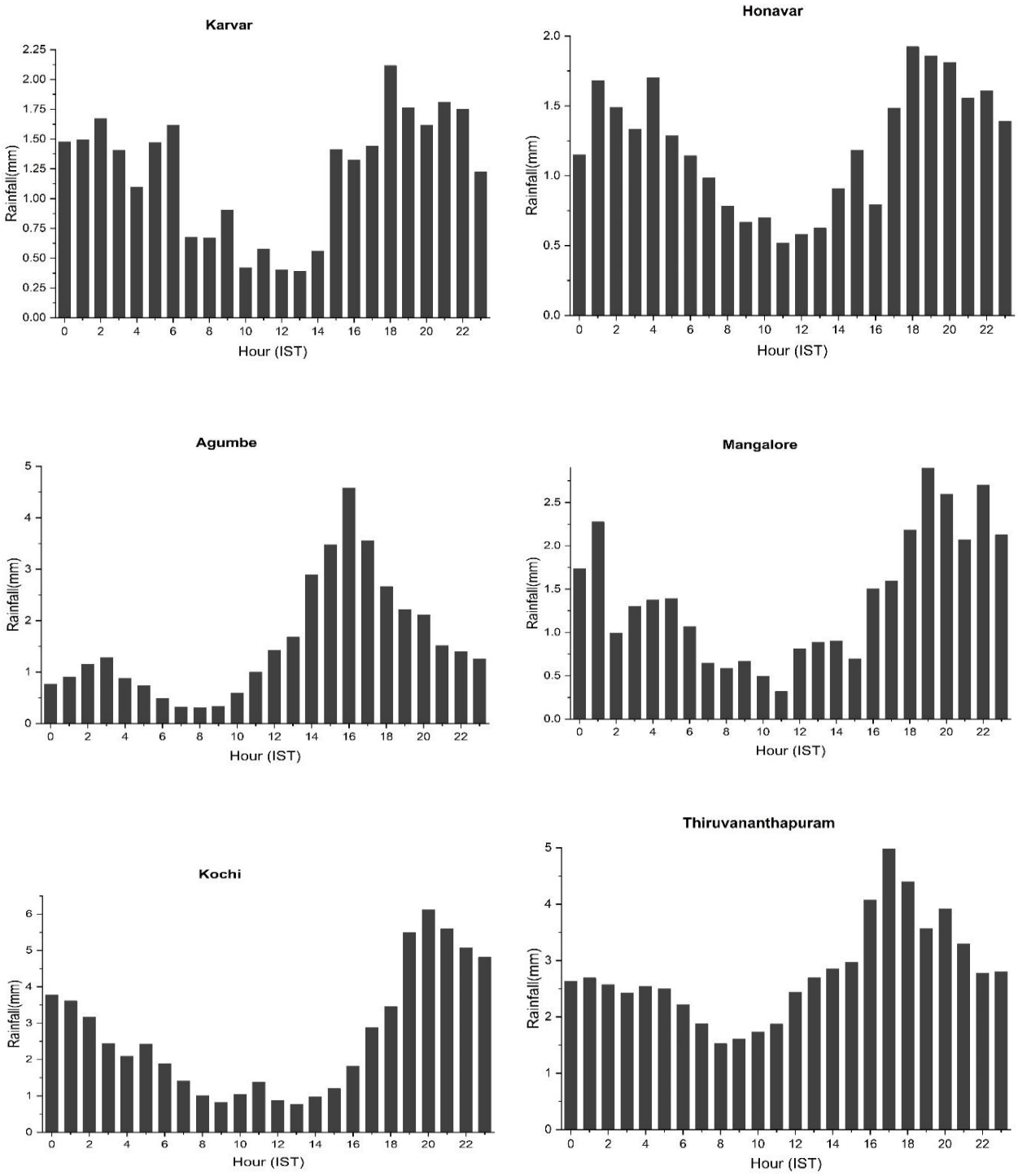

Fig. 6.3. Hourly average rainfall (in mm) during the NE monsoon season (Oct-Dec) showing diurnal variation of rainfall at different stations over south Peninsula. Period: 1969-2021.

Using daily rainfall data from 15 September, 1998 to 15 January 1999, a spectral analysis was made to see the periodicities of rainfall during the NE monsoon season. The results are shown in Fig. 6.6. The spectral analysis shows a strong periodicity of rainfall activity with 30-40 days, which is also statistically significant. Another weaker periodicity is observed around 20 days. Fig 6.6 c shows the wavelet spectrum which also suggests the periodicity around 30-40 days. It may be interesting to note that these two periodicities are predominantly observed during the southwest monsoon season. More studies are required to understand the physical mechanisms of these oscillations during the NE monsoon season. What are the physical mechanisms for these oscillations and what is the predictability of this oscillation?

Sreekala et al., (2018) analyzed intra-seasonal rainfall activity during the NE monsoon season and the combined effect of Madden Julian Oscillation (MJO), NSO and IOD. The study has revealed that the intra-seasonal variation of daily rainfall over the south peninsula during the NEM season is associated with various phases of the eastward propagating MJO life cycle.

A similar study was made using more years of updated data to understand the ISO activity during the NE monsoon season in terms of different phases of MJO. ERA5 (Hersbach et al., 2020) daily precipitation datasets have been used for analyzing the intra-seasonal variation of NE Monsoon rainfall over the Oceanic region. Total hourly precipitation data are used in this study. In addition, zonal and meridional winds at 850 hPa from ERA5 data and Outgoing Long-wave Radiation (OLR) data (Liebmann and Smith 1996) from NCEP/NCAR during 1979-2021 are also used in the current study.

The Real-time Multivariate MJO indices (RMM1 and RMM2) from http://www.bom.gov.au/ bmrc/clfor/cfstaff/matw/maproom/RMM/ were used for defining the various Phases of MJO (Wheeler and Hendon 2004). MJO indices were calculated as the principal component (PC) time series of the two leading empirical

orthogonal functions (EOFs) of combined daily mean fields for 850 and 200 hPa zonal winds and OLR averaged over the tropics (15°S–15°N).

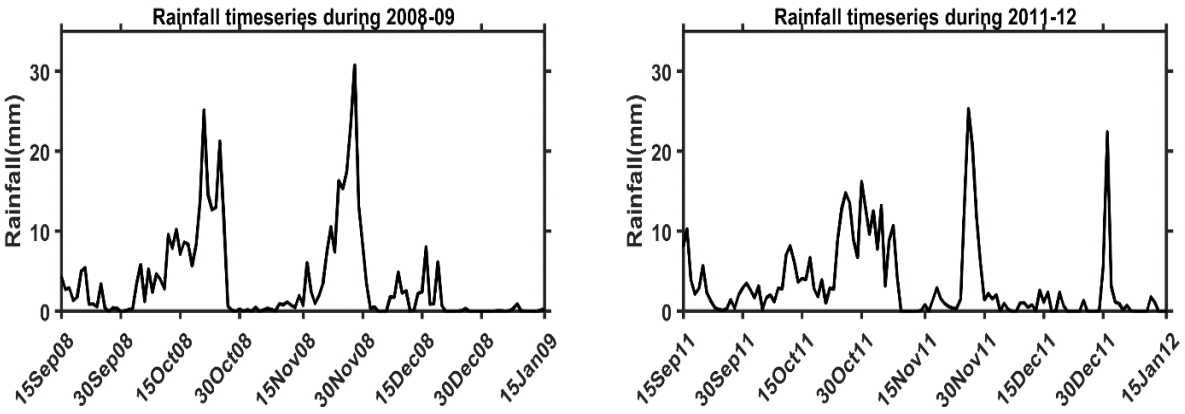

Fig. 6.4. Time series of daily rainfall averaged over NE Monsoon region during 15 September to 15 January a) 2008-2009 b) 2011-2012.

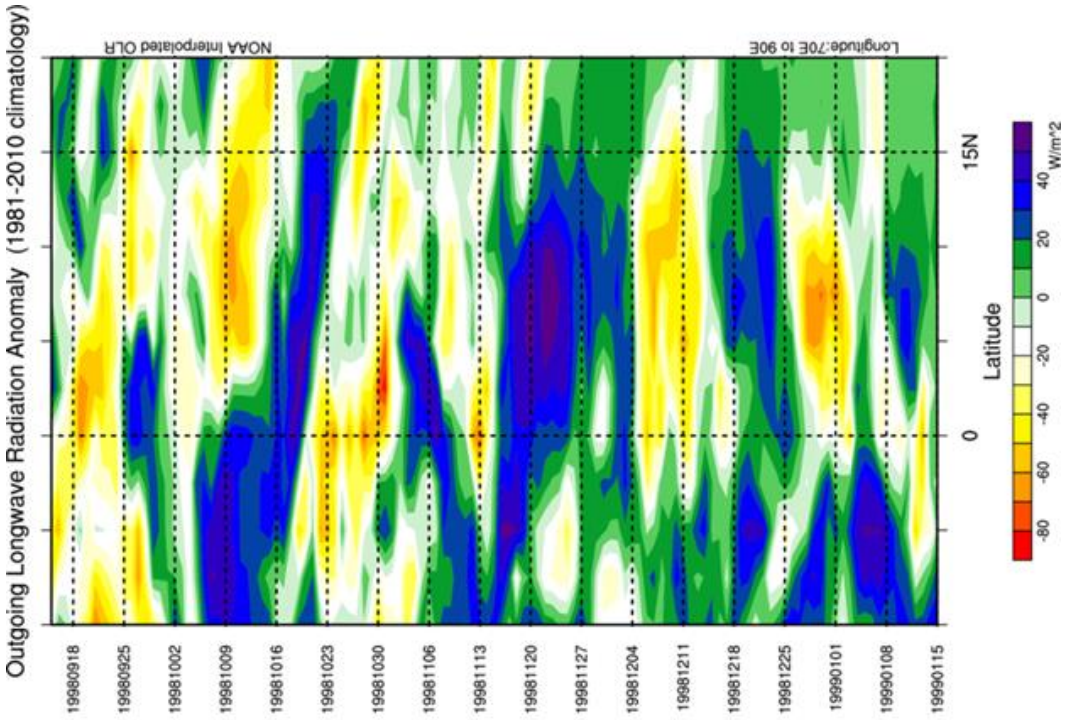

Fig. 6.5 a. Hovmuller diagram (Time vs Latitude) showing northward propagation of convection (OLR anomalies) during 15 September 1998 to 15 January 1999, averaged over 70^0-90^0E.

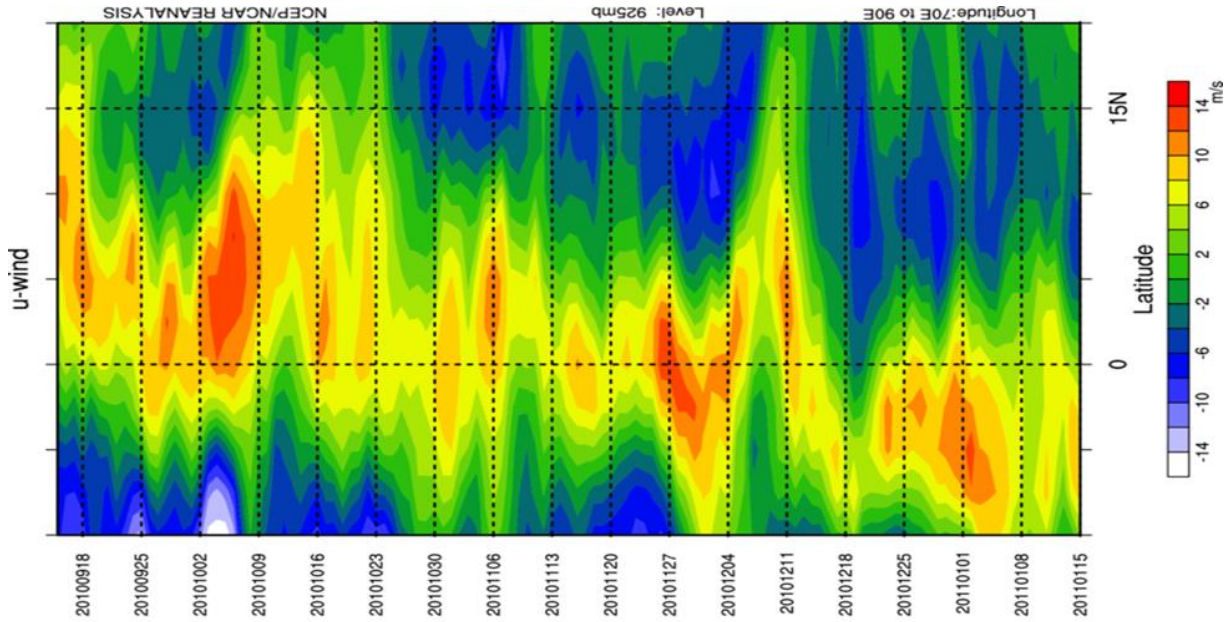

Fig. 6.5 b. Hovmuller diagram (Time vs Latitude) of zonal wind (m/sec) at 925 hPa from 15 September 2010 to 15 January 2011.

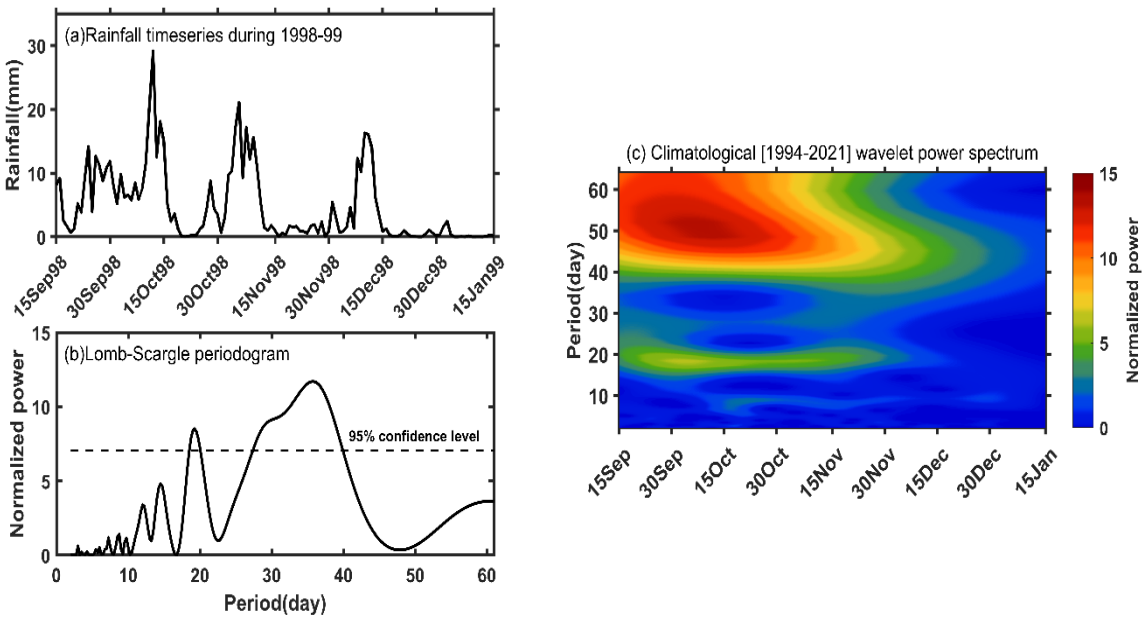

Fig. 6.6. Daily rainfall (in mm) averaged over south Peninsular India from 15 September 1998 to 15 January 1999, b) Lomb-Scargle periodogram of daily rainfall over south Peninsular India from 15 September 1998 to 15 January 1999 and c) wavelet power spectrum of climatological daily rainfall averaged over south peninsular India (1994-2004).

Maps of composite rainfall anomaly (mm) in respect of eight strong phases of MJO superimposed with composite daily OLR anomalies (W/m^{-2}) and composite surface wind vector in the eight strong MJO phases were prepared using the data for the period 1979–2021. The results are shown in Fig. 6.7. Positive rainfall anomaly over south peninsular India and the surrounding Indian Ocean (IO) is observed during the strong MJO phases 2, 3 and 4; and negative rainfall anomaly during the strong MJO phases 6,7 and 8. Therefore, an understanding of the phase of MJO (which is available on real time at http://www.bom.gov.au/) is useful for assessing the prospects of NE monsoon rainfall over the south Peninsula. From Fig. 6.7, it is very clearly seen the northeastward movement of positive rainfall anomalies from the equatorial Indian Ocean to the west Pacific and neighborhood.

Shanmugasundaram et al. (2017) employed hidden Markov model to characterize the spatio-temporal variations of NE monsoon rainfall at pentad time step and its probability of occurrence during 1982–2014. The results indicated the dominant presence of three rainfall states during the season, which were the wet (State-1), coastal wet (State-2), and dry (State-3) states. Seasonal total NEIMR was significantly and positively correlated with the frequency of State-1, whereas it was negatively correlated with that of State-3, indicating a crucial role of the rainfall states in determining water requirements in the southeastern peninsular India. Wet conditions were characterized by enhanced cyclonic activities and increased moisture convergence at 850 hPa over the southeastern peninsular India and its neighbouring oceanic regions (Bay of Bengal and Indian Ocean).

In contrast, dry conditions were associated with anticyclonic circulation and reduced moisture convergence at 850 hPa. The study by Somenath Dutta et al. (2016) revealed that the transition from weak phase to strong phase of north-east monsoon is associated with an enhancement in conversion of zonal potential energy to zonal kinetic

energy, implying a strengthening of Hadley circulation, favouring the above transition. It is also observed that the transition from weak phase to strong phase is associated with enhanced baroclinic energy conversion.

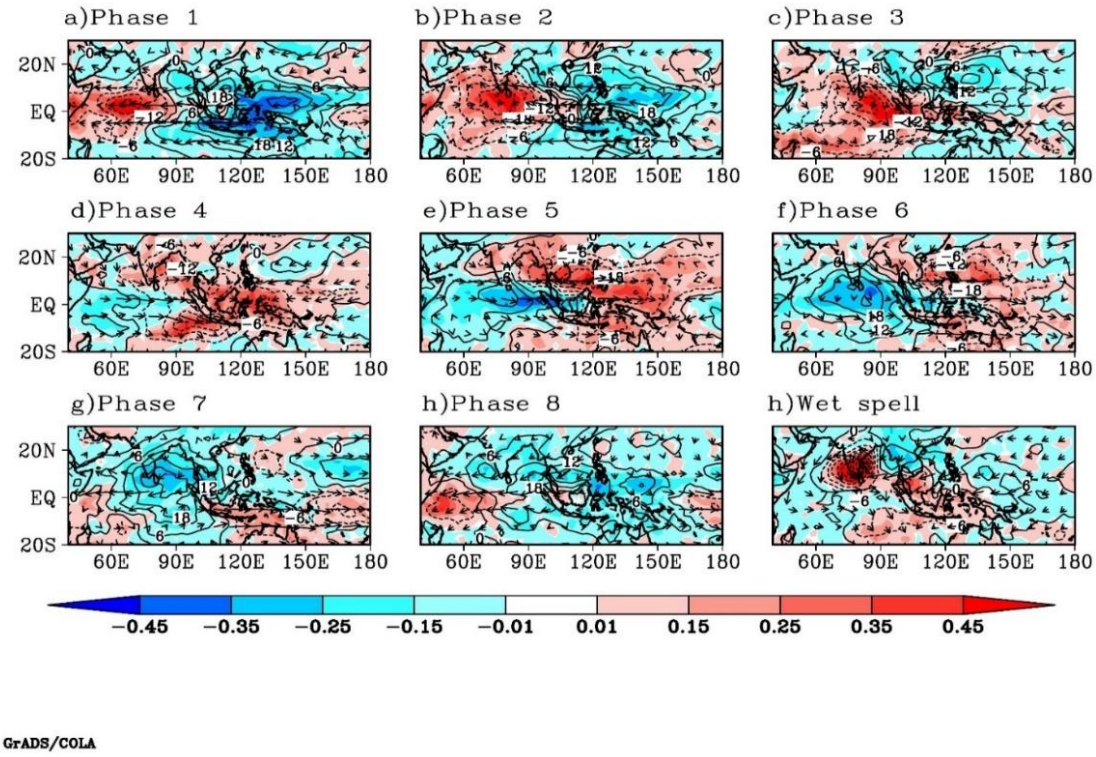

Fig. 6.7. Maps of composite rainfall anomaly (mm) (shaded) in respect of eight strong phases of MJO superimposed with composite daily OLR anomalies (W/m^2) (lines) and composite surface wind vectors in the eight strong MJO phases and during wet spell using the data for the period 1979–2021.

6.2.1. **Active and Weak Spells of NE Monsoon**

Understanding of the intra-seasonal aspects of the NE monsoon is very important for prediction of rainfall. It is well known that the southwest monsoon season exhibits strong active and break spells during the season, and extensive analyses of monsoon active and break spells have been made. During southwest monsoon season, there are active and break spells, with specific characteristics (Ramaswamy 1969, Gadgil and Joseph, 2003 and Rajeevan et al. 2010). It was shown that the total number of active

and break spells during the season is statistically well correlated with the monsoon seasonal rainfall (Rajeevan et al. 2010). Larger number of break spells during the season could lead to a deficient monsoon. However, similar studies of active and break spells during the NE monsoon are unavailable. Since the earlier discussions suggest that there is strong intra-seasonal activity during the NE monsoon season, it is important to understand the active and break spells during the NE monsoon season. A similar analysis of active and weak spells during the NE monsoon season was carried out and the results are discussed below.

Using the IMD gridded daily rainfall data, an area averaged (8-14^0 N, 80-85^0 E) daily rainfall time series is prepared from 01 Oct to 31 Dec. Using the daily rainfall data, standardized rainfall is calculated for all these days from 1981-2021. An Active (wet) Spell is considered when the area averaged standardized rainfall is more than 1.0 for consecutively three days. Similarly, the weak (dry) spell is considered when the area averaged standardized rainfall is less than -0.8. The asymmetry in the threshold of standardized rainfall anomaly was made to ensure active and weak spell days are similar on a long-term climatological data. Using these criteria, active and weak spells during Oct-Dec are identified for the period 1981-2021. These criteria are similar to the criteria for the active and break events adopted for the southwest monsoon season (Rajeevan et al. 2010).

Table 6.1 shows the active and weak spell days during the period 1981-2021, identified using the above criteria.

The time series of total number of active and weak days during the season, year-wise is given in Fig. 6.8. The mean number of active (weak) days during the season is 7.07 (6.56) with a standard deviation of 5.89 and 6.08 respectively. The standard deviation of active and weak spells is very large. There are few years in which there is neither active nor weak spells. In 2003, maximum number of active days (24) was observed. In 1988 and 2016, maximum number of weak days (20) was observed. As

observed during the southwest monsoon season, total number of active and weak spells during the season influence the NE Monsoon seasonal rainfall. The correlation coefficient between the active and weak days during the season with the seasonal rainfall is 0.447 and -0.603 respectively, which are statistically significant at 95% significance level. Total number of weak days is more correlated with the seasonal rainfall, compared to the total number of active days.

Table 6.1

Active and Weak Spells during the NE Monsoon Season (Oct-Dec).

Period 1981-2021

Year	Active Days	Weak Days
1981	25-28 Oct, 02-04 Nov	11-17 Oct, 21-23 Nov
1982	26-28 Oct, 03-05 Nov	01-13Oct
1983	21-27 Dec	11-13Nov
1984	NIL	16-20 Oct, 31 Oct-4Nov
1985	01-03 Oct, 05-11 Oct	19-23 Oct
1986	05-07Nov,12-14Dec	20-25 Oct
1987	16-20 Oct	
1988	22-25Dec	11-18 Oct, 20-23 Oct, 27-31 Oct, 21-23Nov
1989	NIL	03-05 Oct, 14-16 Oct
1990	25-28Oct, 31Oct-2Nov,15-17Dec, 28-31Dec	7-9 Nov
1991	29-31Oct,15-18Nov,24-26Dec	NIL
1992	13-18 Nov,	20-31 Oct
1993	8-12Nov, 4-7 Dec	NIL
1994	04-06 Oct,7-9 Dec ,27-29 Nov	NIL
1995	NIL	NIL
1996	02-05 Oct,18-20 Oct,9-11 Dec, 13-17Dec	2-6 Nov
1997	8-10Nov, 24-30 Nov, 4-10 Dec	07-9 Oct
1998	11-18Oct, 7-10 Nov,8-12 Dec	NIL
1999	5-8Oct, 21-23 Nov	1-3Nov
2000	NIL	25-27 Oct,30Oct-9Nov
2001	NIL	NIL

2002	13-16 Oct	1-8 Oct,21-25 Oct
2003	6-8 Oct,21-24 Oct,1-17 Dec	11-13 Oct,15-17oct,2-6Nov
2004	3-5 Oct	3-5 Nov
2005	12-15 Oct,22-25 Nov	6-8 Oct
2006	26-30oct,4-6dec	12-14 Oct
2007	19-21 Dec	9-13 Oct
2008	24-30 Nov,19-21 Dec	1-3 Oct, 29 Oct-7 Nov
2009	1-5 Oct, 5-12 Nov, 14-16 Nov	10-12 Oct ,14-28 Oct
2010	31Oct-2 Nov ,17-19 Nov,21-23 Nov, 7-9 Dec	11-14 Oct
2011	NIL	1-3 Oct, 5-9 Oct,18-21 Oct, 21-23 Nov
2012	1-3 Nov	8-10 Oct,26-28 Oct
2013	22-26 Oct	9-11 Nov
2014	26-28 Oct	2-5 Oct
2015	30 Nov-3 Dec	16-18 Oct,21-24 Oct
2016	NIL	15-20 Oct,22-29 Oct, 6-8 Nov,11-13Nov
2017	NIL	17-19 Oct,23-26 Oct
2018	NIL	26-31 Oct,6-8Nov
2019	19-22 Oct, 24-26 Oct, 30Nov-3Dec, 13-15 Dec	NIL
2020	11-15 Oct,16-18 Nov, 3-5 Dec,7-9 Dec,	30 Oct-2 Nov
2021	17-19 Oct,12-15 Nov,18-21 Nov	NIL

To understand better the active and weak spells during the NE monsoon season, an analysis is made to make the composites of circulation and SST anomalies for the active and weak spells using the days of active and weak spells mentioned in Table 6.1. The results are discussed below.

Fig. 6.9 shows the composite rainfall anomalies during the active and weak spell days, calculated using the rainfall data of ERA5. Fig. 6.9 shows large positive (negative) anomalies over the south peninsula during the active (weak) spell days. Over the equatorial south Indian Ocean and the west Pacific, there are sharp differences between the active and weak spell days. An active (weak) spell is also associated with suppressed (enhanced) rainfall activity over the west Pacific and the equatorial Indian Ocean.

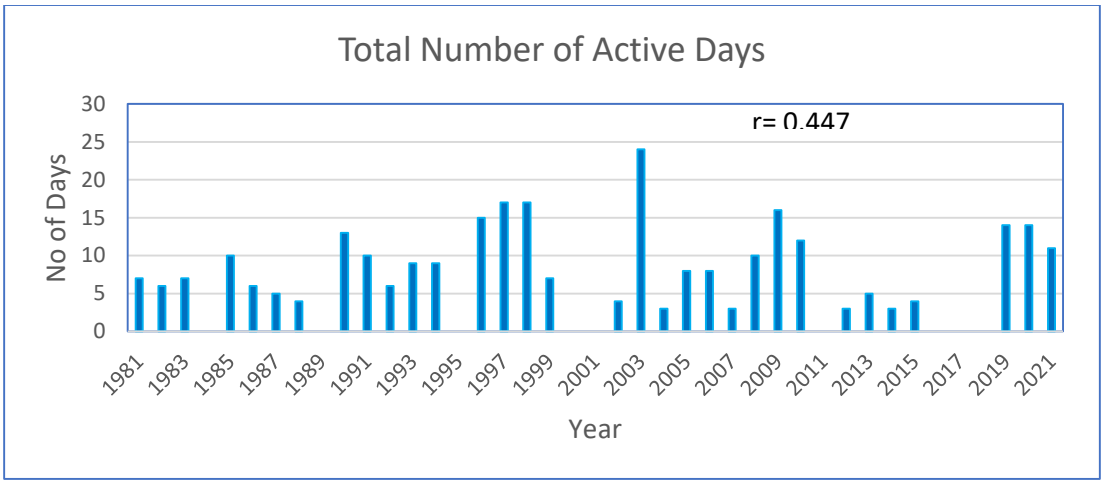

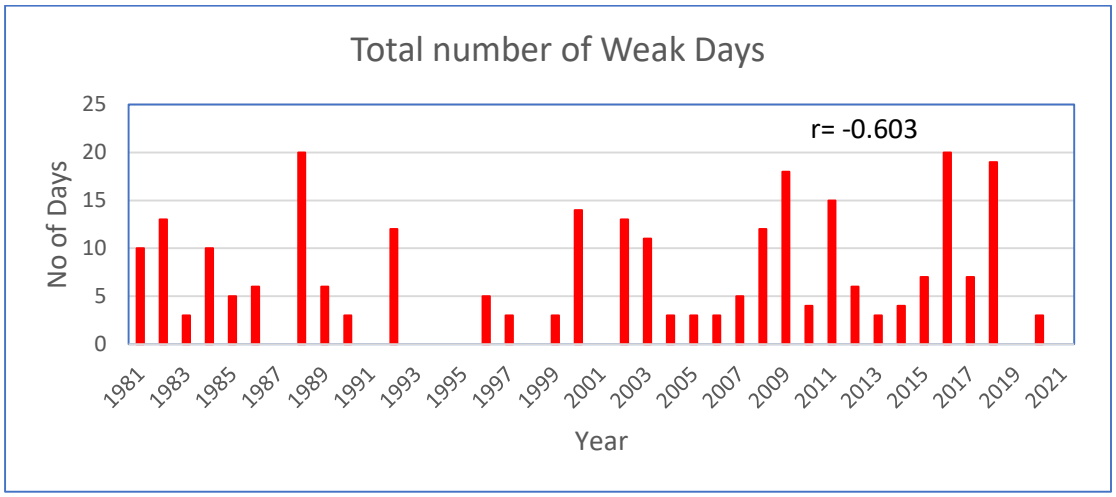

Fig. 6.8. Total number of active (above) and weak (below) days during the OND season for different years, 1981-2021. The correlation coefficient between the total number of active and weak days with the seasonal rainfall is shown in the plots.

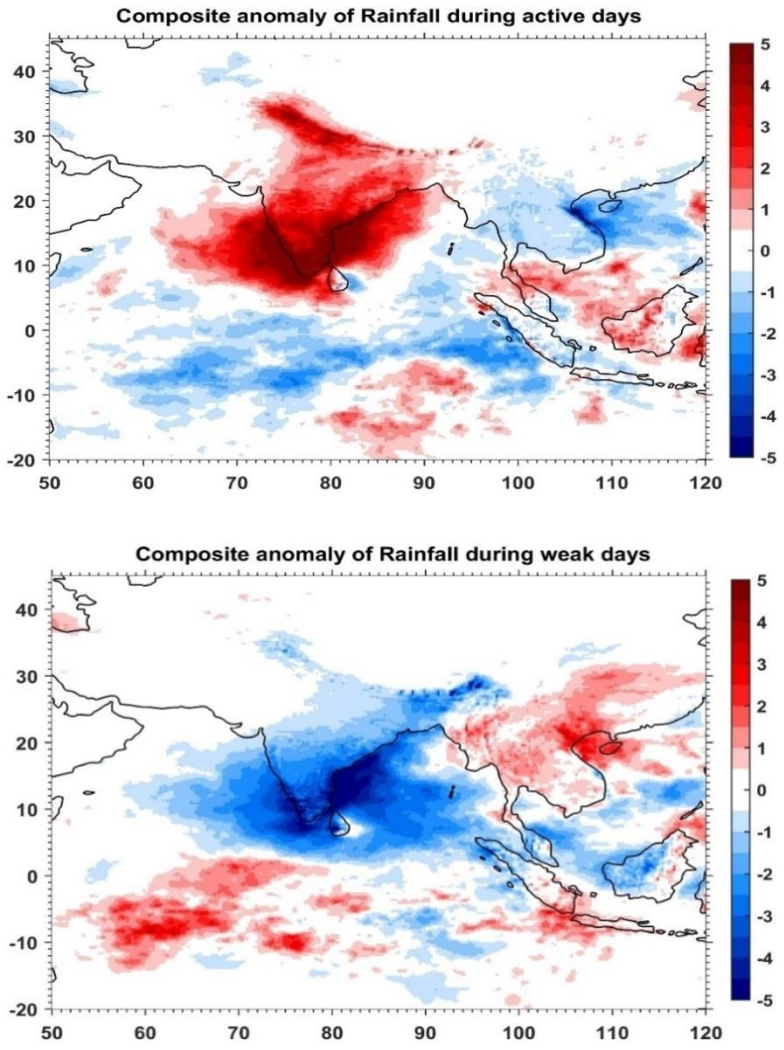

Fig. 6.9. Composite rainfall anomalies (mm) during the active spell days (above) and weak spell days (below) for the period 1981-2021.

Fig. 6.10 shows the composite SST anomalies during the active and weak spell days. The largest differences between the active and weak spells are observed over the equatorial Pacific and the north Indian Ocean. Over the equatorial Pacific Ocean, the SST anomalies are positive (negative) during the active (weak) spells. This indicates that enhanced rainfall activity (more active days) is observed during the El Nino years. Similarly, during the La Nina years, the weak spell days are more. During the active (weak) spell days, SST anomalies over the equatorial Bay of Bengal and Arabian Sea are

large negative (positive). However, over the north Bay of Bengal, positive (negative) anomalies are observed during the active (weak) spell days.

Fig. 6.11 shows the similar composite plots, but for the OLR anomalies. The results are consistent with the rainfall anomaly plots. During the active (weak) spell days, OLR anomalies are large negative (positive) over the Indian sub-continent suggesting enhanced (suppressed) rainfall activity. The drastic difference between these two cases is observd over the west Pacific Ocean and China and adjoining area. During the active (weak) phase of the monsoon, convection over the west pacific is suppressed (enmhanced). The enhanced convection over the west Pacific could cause anomalous descending motion over the Indian region and thus reduce the NE monsoon activity.

Fig. 6.12 shows the 850 hPa wind anomalies during the active and weak spells of NE monsoon. The most striking feature of the wind anomalies is observed over the Indian region. The active (weak) phase of the NE monsoon is associated with cyclonic (anti-cyclonic) circulation anomalies over the Indian region, which is consistent with the observed rainfall anomalies. The other significant anomalies are observed over the west Pacific and adjoining eastern parts of China. During the active (weak) phase, an anomalous anticyclonic (cyclonic) circulation is observed over the region, suggesting below (above) normal convection over the region. This is consistent with the OLR anomalies discussed above.

6.3. **Interannual variation of NE monsoon rainfall (NEMR)**

In this section, the inter-annual variability of NE monsoon rainfall is discussed. There are not adequate studies examining the inter-annual variability of NE monsoon rainfall except the studies by De and Mukhopadhyay, 1999; Kripalani and Kumar, 2004; Raj and Geetha, 2008; Zubair and Ropelewski, 2006; Kumar et al., 2007; Sreekala et al., 2012, Rajeevan et al., 2012.